Kidney International, Vol. 58 (2000), pp. 1797–1804

TECHNICAL NOTE

Progressive adriamycin nephropathy in mice: Sequence of histologic and immunohistochemical events

YANG WANG, YI PING WANG, YUET-CHING TAY, and DAVID C.H. HARRIS

Department of Renal Medicine, University of Sydney at Westmead Hospital, Westmead, Australia

Progressive adriamycin nephropathy in mice: Sequence of histologic and immunohistochemical events.

Background. As an experimental analogue of human focal glomerular sclerosis (FGS), adriamycin (ADR)-induced nephropathy is well-characterized in rats. Previously, this model has not been fully established in mice. The extension of this model to the mouse would be useful in the application of genetic and monoclonal antibody technology to characterize mechanisms of progressive renal disease. Herein, we describe a stable and reproducible murine model of chronic proteinuria induced by ADR.

Methods. Male BALB/c mice were intravenously injected with a single dose of ADR (10 to 11 mg/kg). Seven mice were sacrificed at weeks 1, 2, 4, and 6. Renal function, quantitative morphometric analysis, and electron microscopic studies were performed. Peripheral $CD4^+$ and $CD8^+$ T cells were evaluated using flow cytometric analysis of splenocytes. The leukocytic inflammatory pattern was analyzed by immunohistochemical examination.

Results. Overt proteinuria was observed from day 5 and remained significantly elevated throughout the study period. A focal increase in reabsorption droplets in tubular cells appeared at weeks 1 and 2, and numerous intraluminal casts were present after two weeks. Glomerular vacuolation and mild FGS appeared at week 4. At week 6, extensive focal and even global glomerular sclerosis, associated with moderate interstitial expansion and severe inflammation, were observed. A prominent macrophage infiltration appeared within both interstitium and glomeruli at week 2, followed by accumulation of both $CD4^+$ and $CD8^+$ T cells in interstitium but not glomeruli. There were almost no B lymphocytes seen at any time.

Conclusion. This model should be useful in unraveling the pathogenesis of glomerular and interstitial inflammation and fibrosis in chronic proteinuric renal disease.

Experimental focal glomerular sclerosis (FGS) can be induced by both immunologic and nonimmunological methods. Most nonimmunological procedures, such as the administration of aminonucleoside [1, 2], protein overload [3, 4], partial nephrectomy [5, 6], and the administration of adriamycin (ADR) [7–9], have been described in rats. Among these, the ADR-induced nephropathy model is considered to be an experimental analogue of human minimal lesion nephrotic syndrome and FGS [7, 9]. Furthermore, a long-term study of this model in rats demonstrated severe renal damage with features characteristic of chronic progressive renal disease in humans [9, 10]. Although ADR-induced chronic nephropathy has been well characterized in rats for some time, this model has not been fully established in the mouse [11, 12]. A recent report from Chen et al described experimental FGS in BALB/c mice induced by ADR, with an observation period extended only to 18 days [13].

The present study was designed to establish and characterize a stable and reproducible murine model of chronic progressive nephropathy with significant and persistent proteinuria using ADR. Such a murine model carries the special advantages of economy and the potential for application of genetic and monoclonal antibody manipulation to study pathogenesis.

METHODS

Male BALB/c mice weighing 20 to 25 g and aged eight weeks were obtained from the Animal Care Facility, Westmead Hospital (NSW, Australia). Dose-finding studies defined an optimal dose of 10 to 11 mg/kg body wt of ADR (Doxorubicin Hydrochloride; Pharmacia & Upjohn Pty Ltd., Perth, Australia). ADR was injected once via the tail vein of each nonanesthetized mouse. Seven age-matched male BALB/c mice were injected with same volume of isotonic saline. All control and experimental mice were housed individually, and once a week, a 12-hour collection of spontaneously voided urine was made from each animal. Body weight, urine volume, and urinary protein were measured weekly. Seven mice treated with ADR were sacrificed at weeks 1, 2, 4, and 6. Blood samples for serum albumin and

Key words: glomerulosclerosis, proteinuria, tubulointerstitial fibrosis, inflammation.

Received for publication November 22, 1999
and in revised form March 7, 2000
Accepted for publication April 25, 2000

Table 1. Monoclonal antibodies (mAbs) used in FACS and immunohistochemical staining

Clone	Target molecule	Specificity	Reference
RM4–5	Murine L3T4	MHC class II-restricted T lymphocytes, including most T helper cells	[15]
53–6.7	Murine Ly-2	MHC class I-restricted T lymphocytes, including most T suppressor/cytotoxic cells	[16]
M3/84	Murine Mac-3	Tissue macrophages, some myeloid cell lines, but not lymphocytes or monocytes	[17]
RA3-6B2	Murine CD45R/B220	Pan-B lymphocytes marker, at all stages from pro-B through mature and activated B cells	[18]

All antibodies were purchased from Pharmingen Company (Becton Dickinson and Company, New Jersey, USA). FACS is fluorescence-activated cell sorter.

creatinine were obtained by cardiac puncture under anesthetic (ketamine/xylazine, 100/8 mg/kg body weight), and then animals were completely exsanguinated via the abdominal aorta to minimize the number of circulating inflammatory cells remaining in harvested kidney and spleen. Kidney weight and body weight were measured immediately. All kidney and spleen specimens were processed without delay.

Plasma and urinary creatinine were analyzed using a BM/Hitachi 747 analyzer (Tokyo, Japan). Total urinary protein was quantitatively determined using the Bio-Rad protein assay (Bio-Rad Laboratories, Hercules, CA, USA) according to the manufacturer's instructions in a DU-68 Spectrophotometer (Beckman Instrument, Inc., Irvine, CA, USA), for which purified bovine serum albumin (BSA; Sigma Chemical Company, St. Louis, MO, USA) at concentration ranges 0.2 to 1.5 mg/mL was used as a reference standard. Urine samples were also examined for hematuria and leukocyturia using the Reagent Strips for Urinalysis (Bayer Australia Ltd., Pymble NSW, Australia).

A piece of renal tissue was placed in 10% neutral-buffered formalin fixative at room temperature for 12 hours, embedded in paraffin, evaluated using 4 μ sections, and stained with periodic acid-Schiff (PAS), hematoxylin and eosin (HE), and Masson's trichrome. Quantitative evaluation of FGS, tubular and interstitial lesions was performed using an image analysis system (Optimas 5.23; Optimas Corporation, Seattle, WA, USA) as described previously [14]. Mean values were calculated from each of 20 glomeruli or tubules or 10 random cortical regions per section.

For electron microscopy, kidney specimens were fixed in modified Karnovsky's fixative buffer for two hours, washed two times in 0.1 mol/L MOPS buffer, and then postfixed in 2% buffered osmium tetroxide. After dehydration in a graded ethanol series, specimens were embedded in epoxy resin. Ultrathin sections were stained with uranyl acetate and lead citrate and examined in a Philips CM201s electron microscope.

The sources and specificities of monoclonal antibodies (mAbs) used for fluorescence-activated cell sorter (FACS) analysis are listed in Table 1 [15–18]. The FACS staining procedures used were modified slightly from those previously reported [19]. Briefly, spleen cell suspensions were made in RPMI 1640 medium (GIBCO BRL Life Technologies Inc., Grand Island, NY, USA) with 10% (vol/vol) fetal calf serum (FCS; Trace Biosciences Pty Ltd., Castle Hill, NSW, Australia) and then separated by centrifugation in 4°C. Red blood cells were lyzed, and the number of viable cells was determined. Three $\times 10^5$ cells in 100 μL of medium were incubated with 10 μL of the relevant antibodies at room temperature for 10 minutes in the dark. Washing twice using phosphate-buffered saline (PBS) with 5% FCS, cells were fixed with 2% (wt/vol) paraformaldehyde and stored in the dark at 4°C until the cells were analyzed using a FACScan (Becton Dickinson). The immunohistochemical (IHC) staining was performed by the following protocol: 5 μ cryostat sections of both kidney and spleen were placed on slides previously coated with 0.01% (wt/vol) of poly-L-lysine (Sigma). Sections were fixed in Zamboni's fixative [20] for 30 minutes at 4°C and then passed through methanol for five minutes and acetone for one minute at −20°C. An avidin-biotin complex (ABC) technique was used. The primary mAbs are also listed in Table 1. The secondary antibody was a biotinylated rabbit anti-rat immunoglobulin (Dako Corporation, Carpinteria, CA, USA). For negative controls, primary antibodies were replaced with equivalent concentrations of normal rat immunoglobulin. All specimens were stained in duplicate. To avoid false negative staining, a spleen section was placed and stained on every slide as a positive control. Brown staining of cells was regarded as positive immunoreactivity. The number of positive cells was evaluated from the mean of five cortical and medullary fields (magnification ×400) in each section.

Two-way analysis of variance was used in all statistical tests. Bonferroni's correction was used for multiple comparison. Results are represented as mean ± SD. A value of P less than 0.05 was considered to indicate statistical significance.

RESULTS

In a series of preliminary experiments, we attempted to induce nephropathy in two different strains of mice:

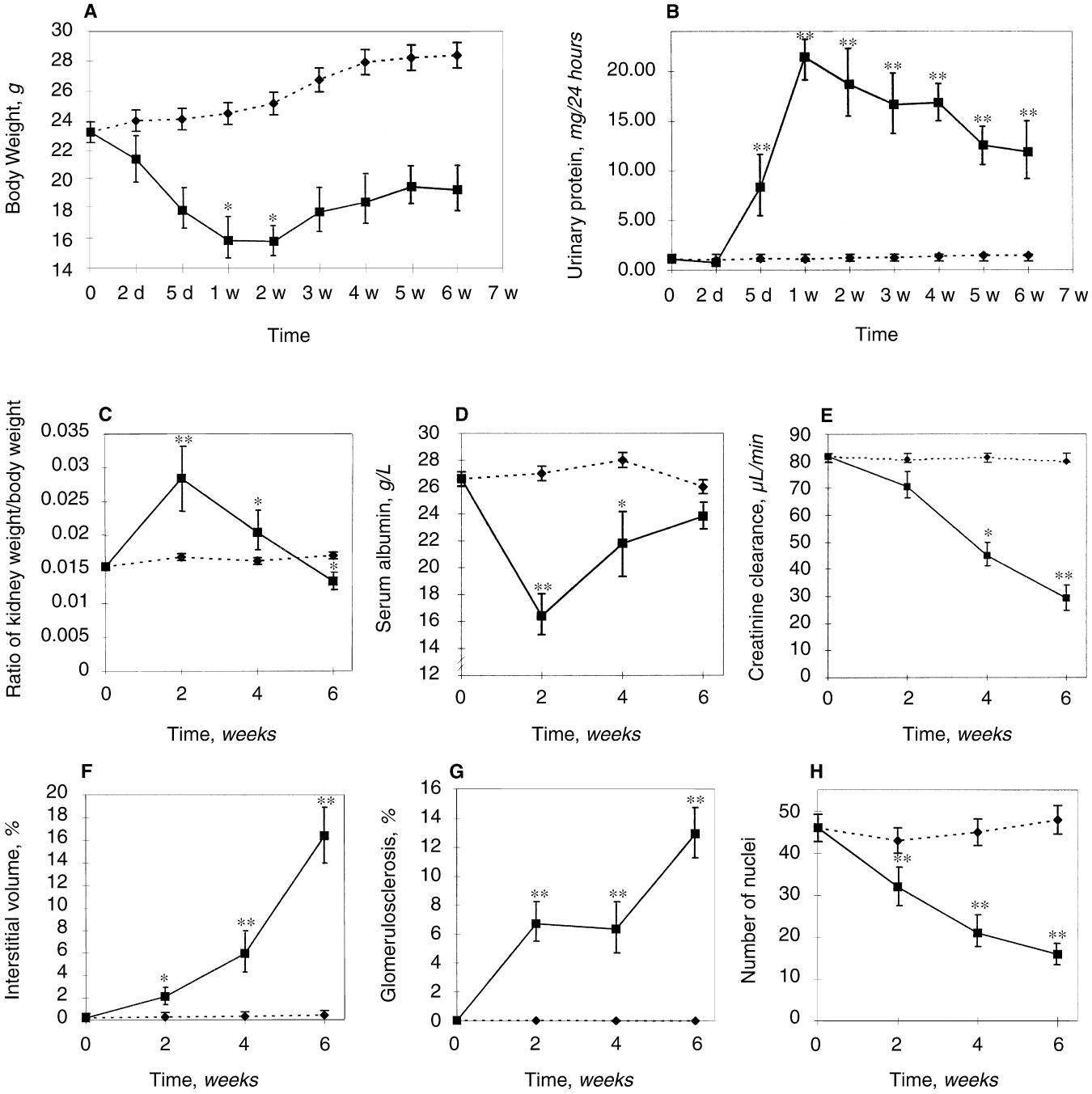

Fig. 1. Mean body weight (*A*), total urinary protein (*B*), ratio of kidney weight/body weight (*C*), serum albumin (*D*), creatinine clearance (*E*), relative interstitial volume (*F*), mean percentage of glomerulosclerosis (*G*), and mean number of nuclei per glomerulus (*H*) for groups with saline-treated (◆) and adriamycin (ADR)-treated (■) mice plotted against time. Values are expressed as means ± SD. $^*P < 0.05$; $^{**}P < 0.01$.

BALB/c and C57BL/6J. C57BL/6J mice either failed to develop any significant proteinuria or histologic change, even at eight weeks after ADR injection of 15 mg/kg body weight or died within two weeks of ADR injection of 20 mg/kg body weight or more. In contrast, in BALB/c mice, a single injection of ADR less than 10 mg/kg body weight or a double injection with a total dosage of up to 14 mg/kg body weight produced an unstable model with wide individual variations. A high dosage of ADR (more than 12 mg/kg body weight) by single injection caused dehydration, gastrointestinal bleeding, or severe hematuria and, in about 25% of experimental mice, severe cachexia, causing death before week 3. A similar phenomenon has also been described by Chen et al [13]. However, in the present study, using an average dosage of 10.5 mg/kg body weight in a 2 mg/mL solution (range

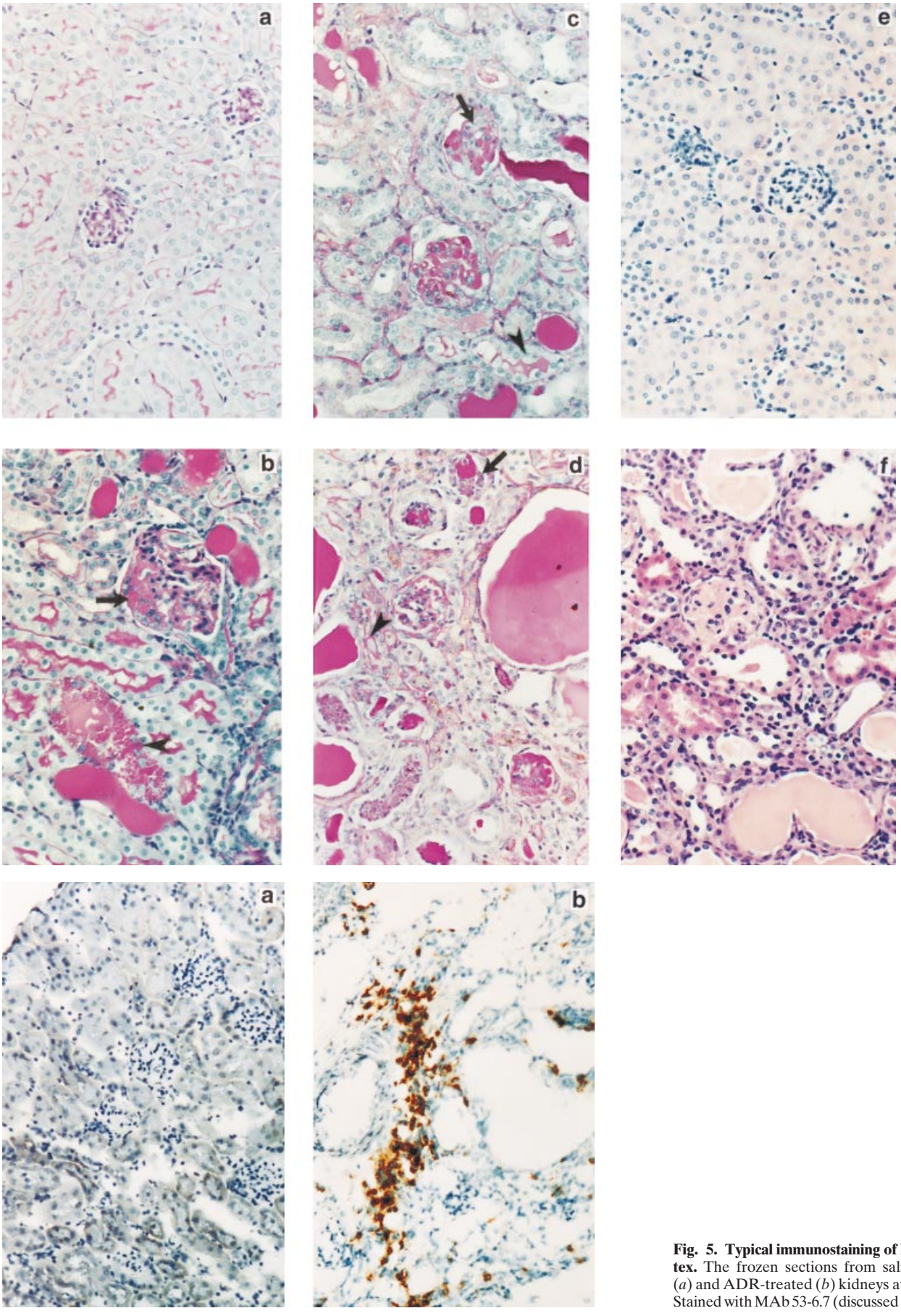

Fig. 5. Typical immunostaining of kidney cortex. The frozen sections from saline-treated (*a*) and ADR-treated (*b*) kidneys at six weeks. Stained with MAb 53-6.7 (discussed in the text).

Fig. 2. (*a*) Saline-treated control mice showed morphologically normal glomeruli and tubules. (*b*) ADR-treated mice at week 2 showed glomerular hypertrophy and hyaline deposits (arrow). Resorption droplets (arrowhead) in tubule cells, as well as intratubular casts, were also found. Some tubules were normal. (*c*) At week 4, mesangial expansion (arrow) in glomeruli, tubular vacuolization (arrowhead), and mild interstitial proliferation were found. Well-developed exudative (fibrin-cap) lesions were also easily seen in glomeruli. (*d*) Global glomerular sclerosis (arrow), tubular collapse (arrowhead), and severe interstitial expansion were seen at week 6. Micrographs a–d were stained by PAS. (*f*) The number of nuclei was reduced in glomeruli and accompanied by a significant interstitial infiltration at week 6, as compared with control (*e*). Both were stained by HE (×400).

10 to 11 mg/kg body weight), all BALB/c male mice treated with ADR developed nephrotic syndrome and remained alive throughout the study period of up to eight weeks.

General characteristics

All experimental animals developed nephropathy characterized by proteinuria, hypoalbuminemia, hypercreatininemia, and progressive renal injury. As shown in Figure 1A, the mean body weight of ADR groups fell quickly after treatment and reached its nadir at week 2, after which body weight increased gradually and more slowly than control. The surface of all kidneys of ADR-treated animals was granular and pale in color in comparison to control. The kidneys were hypertrophied during early nephrosis and atrophied later (Fig. 1C). Overt proteinuria appeared at day 5 and was maximal at day 7. At all time points after one week, high levels of proteinuria were observed in all experimental animals (Fig. 1B). As determined by the Reagent Strips for Urinalysis, 10 of 28 mice (35.7%) had hematuria (graded from 2 to 3+, equivalent to 25 to 80 red blood cells/μL), whereas 15 mice (53.6%) had leukocyturia (graded from 2 to 3+, equivalent to 70 to 125 leukocytes/μL). No control mice had hematuria or leukocyturia at any time point during the study period. ADR treatment produced a marked fall of serum albumin by a median of 39% after one week, after which levels rose gradually but remained persistently lower than control at all times. Creatinine clearance continued to decline with time and was significantly different in comparison with control after week 4 (Fig. 1E).

Morphometric and histopathologic studies

The mean number of cells (Fig. 1H) and relative capillary area in each glomerulus fell throughout the experimental period, coincident with a significant increase in mesangial matrix area. The degree of interstitial volume markedly increased with time (Fig. 1F), indicating the severity of tubular interstitial expansion. Analysis by light microscopy demonstrated the serial changes in experimental kidneys (Fig. 2). At weeks 1 and 2, there was a focal increase in resorption droplets in tubular cells and intraluminal casts. Glomeruli were increased in size, with marked hyaline deposits. At week 4, tubules displayed severe changes, including a decrease in height of tubular epithelial cells, a loss of brush border, and vacuolization. The interstitial volume increased mildly and focally, but there was a moderate interstitial monocyte infiltration. Glomeruli were reduced in size with several vacuoles, collapse of tuft, as well as expansion of the mesangium caused by an increase in PAS-positive material. At week 6, tubular atrophy and intratubular cast formation with tubulointerstitial expansion were widely observed in the cortex. Extensive FGS and severe interstitial fibrosis and inflammation were present. In addition, global sclerosis was observed in many glomeruli.

Electron microscopic study

Ultrastructural examination showed fusion of foot processes of the glomerular epithelial cells in ADR-treated mice. The fusion was segmental at week 1 (Fig. 3) and widespread at week 6 (data not shown). Normal control mice failed to show any epithelial cell abnormality.

FACS and IHC analysis

Peripheral T lymphocytes in spleen were analyzed using a FACScan. The mean percentage of $CD4^+$ and $CD8^+$ cells among total leukocytes in spleen was 37 and 21%, respectively (Fig. 4a), in agreement with the results of other researchers [21, 22]. There were no significant changes in either $CD4^+$ or $CD8^+$ cell numbers at any time point in experimental animals (Fig. 4 b, c). IHC examination of the renal tissue was performed at weeks 2, 4, and 6 after ADR injection. Lymphocytes were rarely seen within interstitium and were never identified in glomeruli of control animals, whereas a small population of macrophages could be found. $CD4^+$, $CD8^+$ T cells, and macrophages was significantly increased in the kidneys of ADR mice. In the earlier stages, macrophage accumulation in the interstitium was prominent, and infiltration in the glomeruli could be readily found. Interstitial macrophages appeared to originate in a sheath surrounding many glomeruli. However, macrophage infiltration dramatically decreased in later stages, accompanied by a gradual increase in the number of T lymphocytes and development of renal injury, including tubular atrophy and interstitial expansion. The number of infiltrating T lymphocytes within the interstitium increased throughout the evolution of the experiment (Table 2).

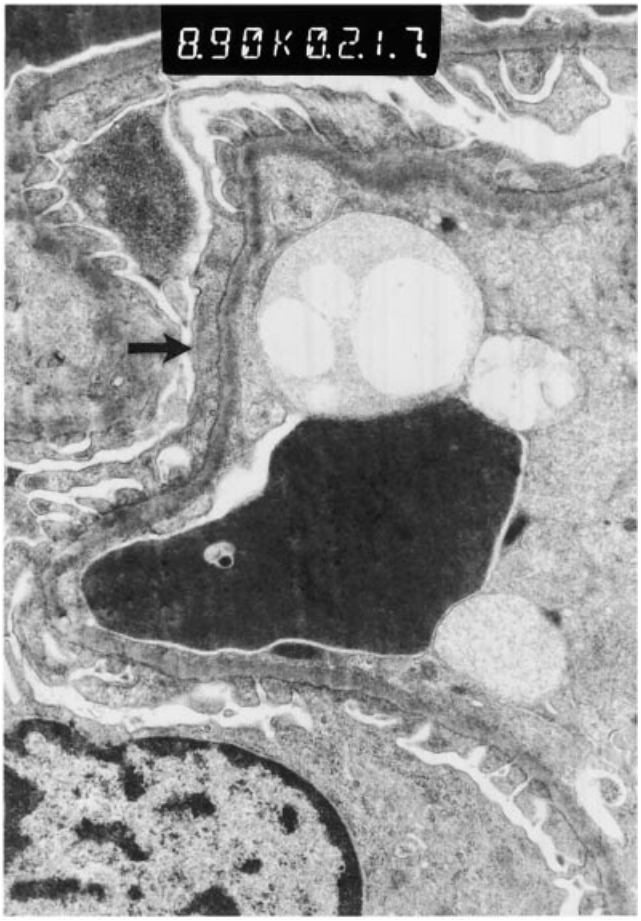

Fig. 3. Ultrastructure of glomerular epithelial cells showed segmental fusion of foot processes (arrow) in ADR-treated mice at week 1 (×17,800).

Both $CD4^+$ and $CD8^+$ cells were greatly increased at week 6 compared with at week 4 ($P < 0.01$), both in cortex and medulla. In contrast, T cells were never identified within the glomerulus at any stage of the experiment. Figure 5 shows the IHC staining of $CD8^+$ cells in kidney cortex. $CD8^+$ cells appeared to migrate from blood vessels and infiltrated the tubulointerstitium (Fig. 4b). No $CD8^+$ cells were seen in glomeruli even though glomeruli were closely surrounded by $CD8^+$ cells. $CD4^+$ cells followed a similar distribution (data not shown). In contrast to T cells and macrophages, few if any B cells were found at any time.

DISCUSSION

Despite an abundance of literature describing chronic nephropathy in rats, no model of chronic glomerular and tubulointerstitial changes induced by ADR has been convincingly established in mice. Extension of this model to the mouse has the potential benefits of application of gene knockout and transgenic mouse technology to characterize the mechanisms of progressive renal disease, and the real advantage of cost savings in terms of animal purchase and maintenance, and use of expensive interventions such as mAbs.

In preliminary experiments, we showed that the murine ADR model could be established in BALB/c but not C57BL/6 mice. The reason for this difference is unknown. Using eight inbred murine strains, Kimura et al reported that BALB/c mice were highly susceptible to nephrosis induced by daunomycin, which has a quite similar structure to ADR, while C57BL/6J was completely resistant to it [23]. They reported that the strain specificity in susceptibility to nephrosis is genetically controlled, involving at least three genes (or clusters of genes). Our experiment showed that BALB/c is a suitable but strictly dose-dependent strain for establishing a stable and reproducible ADR nephropathy model.

In the present studies, overt proteinuria appeared shortly after an intravenous injection of ADR and remained significantly elevated throughout the experimental period. Furthermore, renal pathological, ultrastructural, and functional changes progressed during a long observation period. The renal injury varied with time, and the histologic hallmarks resembled those seen in chronic renal diseases in humans. Interstitial inflammatory cell infiltration is an early event in the development of this murine ADR nephropathy, and the infiltration consists of macrophages and T lymphocytes. The demonstration of initial interstitial infiltration by macrophages at week 2, followed by accumulation of both $CD4^+$ and $CD8^+$ T cells and the disappearance of macrophage infiltration by week 6 as well as a virtual absence of B lymphocytes, is consistent with previous observations in other FGS models [4, 24–29]. The ultimate roles of macrophages and T cells in glomerular and tubulointerstitial injury are still unclear. Macrophages have been shown to mediate acute glomerular injury and to be involved in the stimulation of mesangial cell proliferation and induction of FGS in many experimental models [25–28]. Macrophage-derived products, for example interleukin-1, interleukin-6, tumor necrosis factor-α, platelet-derived growth factor, and transforming growth factor-β, have been associated with glomerular injury and stimulation of mesangial cell proliferation and matrix formation [29]. The immune-activated macrophages may also play an important role in the immunopathogenesis of interstitial fibrosis in glomerulonephritis via a delayed type hypersensitivity mechanism [29]. T lymphocytes also appear to be important in the progression of renal injury. Accumulation and activation of macrophages can be directed by T cells. Tipping, Neale, and Holdsworth proposed that glomerular macrophage infiltration is dependent on T cells [24]. In preliminary experiments, we found that a few $CD4^+$ T cells appeared in juxtamedullary glomeruli in first 24 hours and disap-

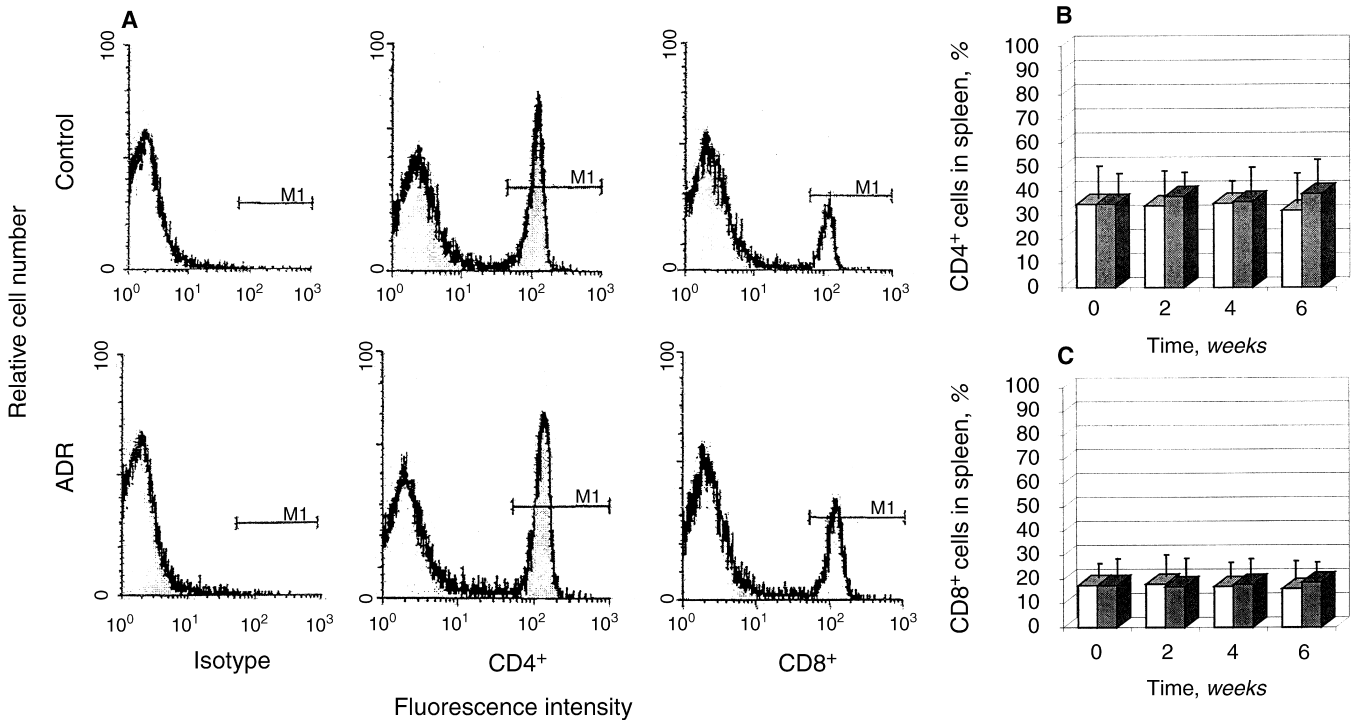

Fig. 4. (*A*) Flow cytometry analysis of peripheral CD4$^+$ and CD8$^+$ cells (in spleen) with FITC-conjugated monoclonal antibodies (mAbs). The *X* axis shows fluorescence intensity and the *Y* axis shows the relative cell number. Age-matched saline controls are shown in the upper panels, and ADR-treated animals at week 6 are shown in the lower panels. Column 1: Background staining with rat IgG 2a, κ isotype standard; column 2: mAb RM4-5 (anti-L3T4); column 3: MAb 53-6.7 (anti-Ly-2). Stained cells were analyzed using the FACS-II with a logarithmic amplifier. (*B* and *C*) Percentage of peripheral CD4$^+$ and CD8$^+$ cells measured by FACS at weeks 0, 2, 4, and 6 after ADR treatment. Symbols are: (■) ADR-treated and (□) saline-treated age-matched groups.

Table 2. Frequency of interstitial CD4$^+$ and CD8$^+$ cells (cell number/400× field) by immunostaining

	CD4$^+$		CD8$^+$	
Week(s)	Cortex	Medulla	Cortex	Medulla
0	1.8 ± 1.5	1.6 ± 1.1	0.2 ± 0.5	0.4 ± 0.6
2	12.4 ± 4.3[a]	12.8 ± 2.6[a]	9.9 ± 1.7[a]	12.3 ± 3.3[a]
4	25.8 ± 7.7[a]	35.0 ± 4.9[a]	20.4 ± 4.1[a]	37.6 ± 6.0[a]
6	148.1 ± 19.6[a,b]	121.0 ± 11.7[a,b]	63.3 ± 9.3[a,b]	101.3 ± 12.0[a,b]

Values are means ± SD.
[a] $P < 0.01$ compared with age-matched normal control
[b] $P < 0.01$ compared with week 4

peared within two days, followed later by macrophage infiltration (unpublished data). This is also consistent with the finding that glomerular T-cell infiltration is only a transient feature of the first three days following the induction of experimental crescentic glomerulonephritis in the rat [25, 30]. Furthermore, immune-activated T cells have been shown to play an important role in the immunopathogenesis of interstitial fibrosis in glomerulonephritis [24, 31].

In conclusion, a stable and reproducible murine ADR model has been established and characterized in present study. This model is likely to prove useful in unraveling the pathogenesis of interstitial and glomerular inflammation and fibrosis in chronic proteinuric renal disease. At present, a project using mAbs for in vivo manipulation of T cell subsets is underway to investigate the linkage between T-cell infiltration and progressive interstitial fibrosis in murine ADR nephropathy.

ACKNOWLEDGMENTS

This study was supported by a grant from the National Health and Medical Research Council of Australia (No. 970721). The authors thank Dr. Ross Boadle, Department of Electron Microscopy at Westmead Hospital, for his invaluable assistance.

Reprint requests to Dr. Yang Wang, Department of Renal Medicine, Westmead Hospital, Westmead, NSW 2145, Australia.
E-mail: yangw@westgate.wh.usyd.edu.au

REFERENCES

1. Grond J, Weening JJ, Elema JD: Glomerular sclerosis in nephrotic rats: Comparison of the long-term effects of adriamycin and aminonucleoside. *Lab Invest* 51:277–285, 1984
2. Diamond JR, Anderson S: Irreversible tubulointerstitial damage associated with chronic aminonucleoside nephrosis. *Am J Pathol* 137:1323–1332, 1990
3. Lalich JJ, Burkholder PM, Paik WC: Protein overload nephropathy in rats with unilateral nephrectomy: A correlative light immunofluorescence and electron microscopical analysis. *Arch Pathol* 99:72–79, 1975
4. Eddy AA: Interstitial nephritis induced by protein-overload proteinuria. *Am J Pathol* 135:719–733, 1989

5. Grond J, Schilthuis MS, Koudstaal J, Elema JD: Mesangial function and glomerular sclerosis in rats after unilateral nephrectomy. *Kidney Int* 22:338–343, 1982
6. Olson JL, Hostetter TH, Rennke HG, Brenner BM, Venkatachalam MA: Altered glomerular permselectivity and progressive sclerosis following extreme ablation of renal mass. *Kidney Int* 22:112–126, 1982
7. Bertani T, Poggi A, Pozzoni R, Delaini F, Sacchi G, Thoua Y, Mecca G, Remuzzi G, Donati MB: Adriamycin-induced nephrotic syndrome in rats: Sequence of pathologic events. *Lab Invest* 46:16–23, 1982
8. O'Donnell MP, Michels L, Kasiske B, Raij L, Keane WF: Adriamycin-induced chronic proteinuria: A structural and functional study. *J Lab Clin Med* 106:62–67, 1985
9. Okuda S, Oh Y, Tsuruda H, Onoyama K, Fujimi S, Fujishima M: Adriamycin-induced nephropathy as a model of chronic progressive glomerular disease. *Kidney Int* 29:502–510, 1986
10. Cameron J: *The Natural History of Glomerulonephritis: Renal Disease.* Oxford, Blackwell Scientific Publications, 1979, p 329
11. Weiher H, Noda T, Gray DA, Sharpe AH, Jaenisch R: Transgenic mouse model of kidney disease: Insertional inactivation of ubiquitously expressed gene leads to nephrotic syndrome. *Cell* 62:425–434, 1990
12. Watanabe Y, Itoh Y, Yoshida F, Koh N, Tamai H, Fukatsu A, Matsuo S, Hotta N, Sakamoto N: Unique glomerular lesion with spontaneous lipid deposition in glomerular capillary lumina in the NON strain of mice. *Nephron* 58:210–218, 1991
13. Chen A, Sheu LF, Ho YS, Lin YF, Chou WY, Chou TC, Lee WH: Experimental focal segmental glomerulosclerosis in mice. *Nephron* 78:440–452, 1998
14. Rangan GK, Wang Y, Tay YC, Harris DC: Inhibition of nuclear factor-kappaB activation reduces cortical tubulointerstitial injury in proteinuric rats. *Kidney Int* 56:118–134, 1999
15. Wu L, Scollay R, Egerton M, Pearse M, Spangrude GJ, Shortman K: CD4 expressed on earliest T-lineage precursor cells in the adult murine thymus. *Nature* 349:71–74, 1991
16. Nakayama K, Nakayama K, Negishi I, Kuida K, Louie MC, Kanagawa O, Nakauchi H, Loh DY: Requirement for CD8, β chain in positive selection of CD8-lineage T cells. *Science* 263:1131–1133, 1994
17. Flotte TJ, Springer TA, Thorbecke GJ: Dendritic cell and macrophage staining by monoclonal antibodies in tissue sections and epidermal sheets. *Am J Pathol* 111:112–124, 1983
18. Ballas ZK, Rasmussen W: Lymphokine-activated killer cells. VII. IL-4 induces an NK1.1+CD8, α+β- TCR-αβ B220+ lymphokine-activated killer subset. *J Immunol* 150:17–30, 1993
19. Goronzy J, Weyand CM, Fathman CG: Long-term humoral unresponsiveness in vivo, induced by treatment with monoclonal antibody against L3T4. *J Exp Med* 164:911–925, 1986
20. Stefanini M, De Martino C, Zamboni L: Fixation of ejaculated spermatozoa for electron microscopy. *Nature* 216:173–174, 1967
21. Ghobrial RR, Boublik M, Winn HJ, Auchincloss HJ: In vivo use of monoclonal antibodies against murine T cell antigens. *Clin Immunol Immunopathol* 52:486–506, 1989
22. Pedrazzini T, Hug K, Louis JA: Importance of L3T4+ and Lyt-2+ cells in the immunologic control of infection with *Mycobacterium bovis* strain bacillus Calmette-Guerin in mice: Assessment by elimination of T cell subsets in vivo. *J Immunol* 139:2032–2037, 1987
23. Kimura M, Takahasi H, Ohtake T, Sato T, Hishida A, Nishimura M, Honda N: Interstrain differences in murine daunomycin-induced nephrosis. *Nephron* 63:193–198, 1993
24. Tipping PG, Neale TJ, Holdsworth SR: T lymphocyte participation in antibody-induced experimental glomerulonephritis. *Kidney Int* 27:530–537, 1985
25. Floege J, Alpers CE, Burns MW, Pritzl P, Gordon K, Couser WG, Johnson RJ: Glomerular cells, extracellular matrix accumulation, and the development of glomerulosclerosis in the remnant kidney model. *Lab Invest* 66:485–497, 1992
26. Diamond JR, Ding G, Frye J, Diamond IP: Glomerular macrophages and the mesangial proliferative response in the experimental nephrotic syndrome. *Am J Pathol* 141:887–894, 1992
27. Pesek-Diamond I, Ding G, Frye J, Diamond JR: Macrophages mediate adverse effects of cholesterol feeding in experimental nephrosis. *Am J Physiol* 263:F776–F783, 1992
28. van Goor H, van der Horst ML, Fidler V, Grond J: Glomerular macrophage modulation affects mesangial expansion in the rat after renal ablation. *Lab Invest* 66:564–571, 1992
29. Nikolic-Paterson DJ, Lan HY, Hill PA, Atkins RC: Macrophages in renal injury. *Kidney Int* 45(Suppl 45):S79–S82, 1994
30. Lan HY, Paterson DJ, Atkins RC: Initiation and evolution of interstitial leukocytic infiltration in experimental glomerulonephritis. *Kidney Int* 40:425–433, 1991
31. Baldridge JR, Barry RA, Hinrichs DJ: Expression of systemic protection and delayed-type hypersensitivity to Listeria monocytogenes is mediated by different T-cell subsets. *Infect Immun* 58:654–658, 1990